J|A|C|S
ARTICLES
Published on Web 08/05/2006

Magnetic Properties of Lanthanide Chalcogenide Semiconducting Nanoparticles

Michelle D. Regulacio, Konrad Bussmann,† Brad Lewis,‡ and Sarah L. Stoll*

Contribution from the Department of Chemistry, Box 571227, Georgetown University, Washington D.C. 20057

Received March 23, 2006; E-mail: sls55@georgetown.edu

Abstract: To understand the importance of the band gap to the magnetic ordering in magnetic semiconductors, we have studied the effect of particle size on the ferromagnetic Curie temperature in semiconducting EuS. We have synthesized capped ~20 nm EuS nanoparticles using a single-source precursor, [Eu($S_2CN^tBu_2$)$_3$Phen] decomposed in trioctylphosphine. The nanoparticles have been characterized by X-ray powder diffraction, TEM, and magnetic susceptibility measurements as a function of temperature and field. The Curie temperature, based on Arrott plots, is depressed by 1−2 K from the bulk value.

Introduction

Magnetic nanoparticles have been of interest for applications in electronic devices[1] and biological systems[2] and raised significant questions about the fundamental properties of magnetic materials in the nanometer size regime.[3] We have been interested in studying the magnetic lanthanide chalcogenides, LnQ (Ln = lanthanide, Q = O, S, Se, Te), as model systems for probing solid-state properties that are likely to be influenced by band gap tuning using particle size. Although magnetic properties have been studied in metallic (Fe, FePt)[4,5] and insulating (for example Fe_2O_3, Fe_3O_4, and spinels MFe_2O_4, M = transition metal)[6] systems, we believe magnetic semiconductors should provide new insight into the question of how solid-state properties evolve with size. In addition, because the properties are governed by the extent of delocalization of *f* electrons, these materials provide an independent probe of *f* orbital overlap and the degree of bonding covalency in lanthanides, an area of current debate.[7]

The europium chalcogenides were intensely studied in the 1970s[8] and continue to be of both theoretical[9] and experimental[10] interest. Initial studies were motivated by applications that utilize the large Faraday[11] and Kerr effects.[12] The potential for using EuS as a "spin filter" has driven recent thin film studies.[13] The europium chalcogenides are part of a general class of materials that exhibit novel coupled phenomena, i.e., pairwise combinations of magnetic, electronic, and optical properties.[14] Magneto-optical, magnetoresistive, and optoelectronic materials are targeted for the development of new electronic devices (such as GMR heads or LEDs). Recently, there has been particular interest in the synthesis and characterization of nanoparticles of EuO and EuS in the search for new luminescent materials.[15,16]

† Present address: Materials and Sensors Branch (6360), Naval Research Laboratory, 4555 Overlook Ave. SW, Washington, DC 20375.

‡ Present address: Department of Chemistry, The Pennsylvania State University, University Park, PA 16802.

(1) Awschalom, D. D.; Flatte, M. E.; Samarth, N. *Sci. Am.* **2002**, *286* (6), 66−73.
(2) Gould, P. *Mater. Today* **2004**, *7* (2), 36.
(3) (a) Majetich, S.; Jin, Y. *Science*, **1999**, *284*, 470. (b) Gambardella, P.; Rusponi, S.; Veronese, M.; Dhesi, S. S.; Grazioli, C.; Dallmeyer, A.; Cabria, I.; Zeller, R.; Dederichs, P. H.; Kern, K.; Carbone, C.; Brune, H. *Science* **2003**, *300*, 1130. (c) Dumestre, F.; Chaudret, B.; Amiens, C.; Renaud, P.; Fejes, P. *Science* **2004**, *303*, 821. (d) Kodama, R. H. *J. Magn. Magn. Mater.* **1999**, *200*, 359−372.
(4) Farrell, D.; Majetich, S. A.; Wilcoxon, J. P. *J. Phys. Chem. B* **2003**, *107*, 11022.
(5) Sun, S.; Murray, C. B.; Weller, D.; Folks, L.; Moser, A. *Science* **2000**, *287* (5460), 1989.
(6) (a) Vestal, C.; Zhang, Z. J. *J. Am. Chem. Soc.* **2003**, *125*, 9828. (b) Vestal, C.; Song, Q.; Zhang, Z. J. *J. Phys. Chem. B* **2004**, *108* (47), 18222. (c) Vestal, C.; Zhang, Z. J. *Chem. Mater.* **2002**, *14* (9), 3817. (d) Huh, Y. M.; Jun, Y. W.; Song, H. T. *J. Am. Chem. Soc.* **2005**, *127* (35), 12387. (e) Wan, S. R.; Zheng, Y.; Liu, Y. Q. *J. Mater. Chem.* **2005**, *15* (33), 3424. (f) Gu, H. W.; Xu, K. M.; Yang, Z. M. *Chem. Commun.* **2005**, *34*, 4270.
(7) (a) Castro-Rodriguez, I.; Olsen, K.; Gantzel, P.; Meyer, K. *J. Am. Chem. Soc.* **2003**, *125* (15), 4565. (b) Jensen, M. P.; Bond, A. H. *J. Am. Chem. Soc.* **2002**, *124* (33), 9870.
(8) Wachter, P. *CRC Crit. Rev. Solid State Sci.* **1972**, *3* (2), 189−238.
(9) (a) Horn, M.; Strange, P.; Temmerman, W. M.; Szotek, Z.; Svane, A.; Winter, H. *Los Alamos National Laboratory, Preprint Archive, Condensed Matter* **2004**, 1−7. (b) Dietl, T. *Los Alamos National Laboratory, Preprint Archive, Condensed Matter* **2004**, 1−7. (c) Ariponnammal, S.; Natarajan, S. *Mod. Phys. Lett. B* **2000**, *14* (24), 843−848. Kunes, J.; Ku, W.; Pickett, W. E. *J. Phys. Soc. Jpn.* **2005**, *74* (5), 1408.
(10) (a) Sakalle, U. K.; Jha, P. K.; Sanyal, S. P. *Bull. Mater. Sci.* **2000**, *23* (3), 233−235. (b) Kasuya, T. *J. Magn. Magn. Mater.* **1999**, *195* (1), 141−147. (c) Gorlitz, D.; Kotzler, J. *Eur. Phys. J. B* **1998**, *5* (1), 37−43.
(11) Thongchant, S.; Hasegawa, Y.; Tanaka, K.; Fujita, K.; Hirao, K.; Wada, Y.; Yanagida, S. *Jpn. J. Appl. Phys., Part 2* **2003**, *42* (7B), L876−L878.
(12) Fumagalli, P.; Schirmeisen, A. *J. Appl. Phys.* **1996**, *79* (8), 5929.
(13) (a) Hao, X.; Moodera, J. S.; Meservey, R. *Phys. Rev. B* **1990**, *42* (13), 8235−8243. (b) Metzke, R.; Nolting, W. *Phys. Rev. B: Condens. Matter* **1998**, *58* (13), 8579−8589. (c) Horn, M.; Strange, P.; Temmerman, W. M.; Szotek, Z.; Svane, A.; Winter, H. *Los Alamos National Laboratory, Preprint Archive, Condensed Matter* **2004**, 1−7.
(14) Wachter, P. *CRC Crit. Rev. Solid State Sci.* **1972**, *3*, 189.
(15) (a) Thongchant, S.; Hasegawa, Y.; Wada, Y.; Yanagida, S. *Chem. Lett.* **2001**, *12*, 1274. (b) Hasegawa, Y.; Thongchant, S.; Wada, Y.; Tanaka, H.; Kawai, T.; Sakata, T.; Mori, H.; Yanagida, S. *Angwe. Chem., Int. Ed.* **2002**, *41* (12), 2073−2075. (c) Hasegawa, Y.; Thongchant, S.; Kataoka, T.; Wada, Y.; Yatsuhashi, T.; Nakashima, N.; Yanagida, S. *Chem. Lett.* **2003**, *32* (8), 706−709.
(16) (a) Thongchant, S.; Hasegawa, Y.; Wada, Y.; Yanagida, S. *J. Phys. Chem. B* **2003**, *107*, 2193. (b) Regulacio, M. R.; Tomson, N.; Stoll, S. L. *Chem. Mater.* **2005**, *17* (12), 3114−3121. (c) Mirkovic, T.; Hines, M.; Nair, P.; Scholes, G. *Chem. Mater.* **2005**, *17*, 3451.

The europium chalcogenides are small band gap semiconductors, which exhibit a variety of magnetic ordering from ferromagnetic (EuO T_C = 66.8 K, EuS T_C = 16.6 K) to antiferromagnetic (EuTe T_N = 9.64 K) and metamagnetic (EuSe, T_N = 4.6 K becomes ferromagnetic at a field of 0.5 GPa).[17,18] One of the advantages of using particle size to study magnetic properties in this system is that the ordering temperature has a clear dependence on the energy gap. Considered almost a textbook Heisenberg ferromagnet,[19,20] models of EuS typically consider the 12 nearest (Z_1) and 6 next-nearest (Z_2) neighbors of the cation fcc lattice. Using the mean field approximation, the Curie temperature can be related to the exchange integrals, J_1 (ferromagnetic coupling) and J_2 (antiferromagnetic coupling) through the equation

$$k_B T_C = \frac{2}{3} S(S+1)[Z_1 J_1 + Z_2 J_2] \quad (1)$$

where T_C is the Curie ferromagnetic ordering temperature, k_B is Boltzmann's constant, $S = {}^7/_2$ for Eu(II) $4f^7$ ($^8S_{7/2}$) ground state, $Z_1 = 12$, and $Z_2 = 6$.[21] The connection between the Curie temperature and the E_g, band gap, is through J_1, an exchange parameter that has the form

$$J_1 = \frac{Ab^2}{E_g^2} \quad (2)$$

where A is a function of intra-atomic exchange ($4f$ valence to 5d conduction band exchange, a measure of the extent of delocalization of f electrons in the conduction band), b is a measure of the orbital overlap, and E_g is the band gap.[22]

Experimentally the relationship between electronic structure and magnetic properties has been investigated using pressure,[23] which unfortunately affects both the orbital overlap and the band gap.[24] Doping has also been used to probe the electronic structure (in particular the energy separation between the $4f$ valence band and the conduction band) and the magnetic properties in the EuQ materials.[25] At low doping levels, increasing the electron concentration causes an oscillation in the Curie temperature as typically found for materials described by the RKKY interaction.[26] Here we have investigated the role of particle size to study the inter-relationship between the band gap and the magnetic properties. Our evidence points to the importance of particle size on the ordering temperature, and we discuss three mechanisms for how this might occur.

Experimental Section

The dithiocarbamate precursors were prepared according to previously published procedures.[27] The EuS nanoparticles were obtained by the dissolution of [Eu($S_2CN^iBu_2$)$_3$Phen] (1.75 g, 1.85 mmol) in trioctylphosphine (TOP, 25 mL) and oleylamine (15 mL), and the solution was heated to 240 °C and held at this temperature for 7.5 h. Initially, the solution was orange-red and began to darken at approximately 70 °C, and finally it was purple-black by the time the temperature reached 240 °C. After 7.5 h the temperature was reduced to 60 °C, and anhydrous methanol (40 mL) was added to the solution. In a glovebox the solution was transferred to a centrifuge tube and centrifuged at 3500 rpm for 40 min. The yellow-green supernatant was discarded, and the black powder was dissolved in anhydrous heptanes (20 mL). Fresh methanol (40 mL) was added to the dark purple solution, and the precipitate was isolated by centrifugation, washed with methanol, and dried in vacuo. Elemental analysis gave C (6.8%), H (1.52%), P (1.83%), and N (<0.5%).

UV−visible spectra were recorded from 200 to 800 nm in acetonitrile on a Perkin Elmer UV−visible spectrometer in quartz cuvettes. Infrared spectra were measured in the range 450−4000 cm^{-1} as pressed pellets in KBr on a Perkin Elmer FTIR. X-ray powder diffraction patterns were obtained using a Rigaku RAPID Curved IP X-ray powder diffractometer with Cu Kα radiation and an image plate detector. Magnetic measurements were made on a QD SQUID from 50 to 5 K in fields ranging from 500 to 5000 Oe. Arrott plots were obtained by calculating isotherms for seven temperatures. For each field, the magnetization was squared (emu^2/g^2) for T_1 = 14.0037(7), T_2 = 14.9966(6), T_3 = 15.9972(3), T_4 = 16.9967(6), T_5 = 17.9970(23), T_6 = 18.9957(8), T_7 = 19.9984(20) K and plotted as a function of H/M (Oe g/emu) (Figure 5). The values of M_s^2 where H/M is zero (for each isotherm) were then graphed as a function of temperature (Figure 6). The M_s^2 vs T plot where M_s^2 goes to zero was used to determine the Curie temperature, T_C = 15.1834(2) K based on a linear regression (squared correlation coefficient of R^2 = 0.9982(1)). Samples were prepared for TEM measurements by dipping carbon-coated copper TEM grids 5 to 6 times into solutions of the nanoparticles, allowing the grids to dry briefly before reimmersion. Images were taken on a JEOL JEM 1200 EXII TEM operated at 80 keV using a high-resolution Tietz F224 camera.

Results and Discussion

Synthesis. The synthetic route to form nanoparticles is extremely important to elucidating properties because the size,[28] shape,[29] and surface properties[30] all have a profound influence over optical and magnetic measurements.[31,32] Previously, EuS nanoparticles have been made by solid-state diffusion of powdered EuS into the pores of zeolites,[33] formation in liquid ammonia solutions,[34] and decomposition from single source precursors[35] or white LED irradiation resulting in uncapped nanoparticles.[36] Unfortunately, surface conditions substantially

(17) Wernick, J. H. In *Treatise on Solid State Chemistry, the Chemical Structure of Solids*; Hannay, N. B., Ed.; Plenum Press: New York, 1974; Vol. 1, pp 175−272.
(18) Fujiwara, H.; Kadomatsu, H.; Kurisu, M.; Hihara, T.; Kojima, K.; Kamigaichi, T. *Solid State Commun.* **1982**, *42*, 509.
(19) Nolting, W. *J. Phys. C: Solid State Phys.* **1982**, *15*, 733−745.
(20) Rhyne, J.; McGuire, T. P. *IEEE Trans. Magn.* **1972**, *8* (1), 105.
(21) (a) Wolf, W. P.; McGuire, T. R.; Shafer, M. W. *J. Appl. Phys.* **1964**, *35* (3), 984. (b) Zinn, W. *J. Magn. Magn. Mater.* **1976**, *3*, 23.
(22) Goodenough, J. B. *Magnetism and the Chemical Bond*; John Wiley and Sons: New York, 1963; pp 144 and 167.
(23) (a) Goncharenko, I. N.; Mirebeau, I. *Phys. Rev. Lett.* **1998**, *80* (5), 1082−1085. (b) Schwob, P.; Vogt, O. *Phys. Lett.* **1967**, *24A*, 242. (c) Fujiwara, H.; Kadomatsu, H.; Kurisu, M.; Hirara, T.; Kojima, K.; Kamagaichi, T. *Solid State Commun.* **1982**, *42*, 509.
(24) Goni, A. R.; Strossner, K.; Syassen, K.; Cardona, M. *Phys. Rev. B* **1987**, *36* (6), 1581.
(25) (a) Holtzberg, F.; McGuire, T. R.; Methfessel, S.; Suits, J. C. *Phys. Rev. Lett.* **1964**, *13* (1), 18−21. (b) Maletta, H. *J. Appl. Phys.* **1982**, *53* (3), 2185. (c) von Molnar, S.; Methfessel, S. *J. Appl. Phys.* **1967**, *38* (3), 959−964. (d) Maletta, H. *J. Appl. Phys.* **1982**, *3* (3), 2185.
(26) Holtzberg, F.; McGuire, T. R.; Methfessel, S.; Suits, J. C. *Phys. Rev. Lett.* **1964**, *13* (1), 18.
(27) (a) Su, C.; Tan, M.; Tang, N.; Gan, X.; Liu, W. J. *Coord. Chem.* **1996**, *38*, 207. (b) Regulacio, M. D.; Tomson, N.; Stoll, S. L. *Chem. Mater.* **2005**, *17*, 3114.
(28) Alivisatos, A. P. *Science* **1996**, *271*, 933.
(29) Xia, Y.; Yang, P.; Sun, Y.; Wu, Y.; Mayers, B.; Gates, B.; Yin, Y.; Kim, F.; Yan, H. *Adv. Mater.* **2003**, *15* (5), 353−389.
(30) Kalyuzhny, G.; Murray, R. *J. Phys. Chem. B* **2005**, *109*, 7012−7021.
(31) (a) Cheon, J.; Kang, N.-J.; Lee, S. M.; Lee, J.-H.; Yoon, J.-H.; Oh, S. J. *J. Am. Chem. Soc.* **2004**, *126*, 1950−1951. (b) Seo, W. S.; Jo, H. H.; Lee, K.; Kim, B.; Oh, S. J.; Park, J. T. *Angew. Chem., Int. Ed.* **2004**, *43*, 1115. (c) Song, Q.; Zhang, J. Z. *J. Am. Chem. Soc.* **2004**, *126*, 6164.
(32) Zhao, F.; Sun, H.-L.; Gao, S.; Su, G. *J. Mater. Chem.* **2005**, *15*, 4209.
(33) Chen, W.; Zhang, X.; Huang, Y. *Appl. Phys. Lett.* **2000**, *76* (17), 2328−2330.
(34) Thongchant, S.; Hasegawa, Y.; Wada, Y.; Yanagida, S. *J. Phys. Chem. B* **2003**, *107*, 2193−2196.
(35) (a) Regulacio, M. R.; Tomson, N.; Stoll, S. L. *Chem. Mater.* **2005**, *17* (12), 3114−3121. (b) Mirkovic, T.; Hines, M.; Nair, P.; Scholes, G. *Chem. Mater.* **2005**, *17*, 3451
(36) Hasegawa, Y.; Afzaal, M.; O'Brien, P.; Wada, Y.; Yanagida, S. *Chem. Commun.* **2005**, 242−243.

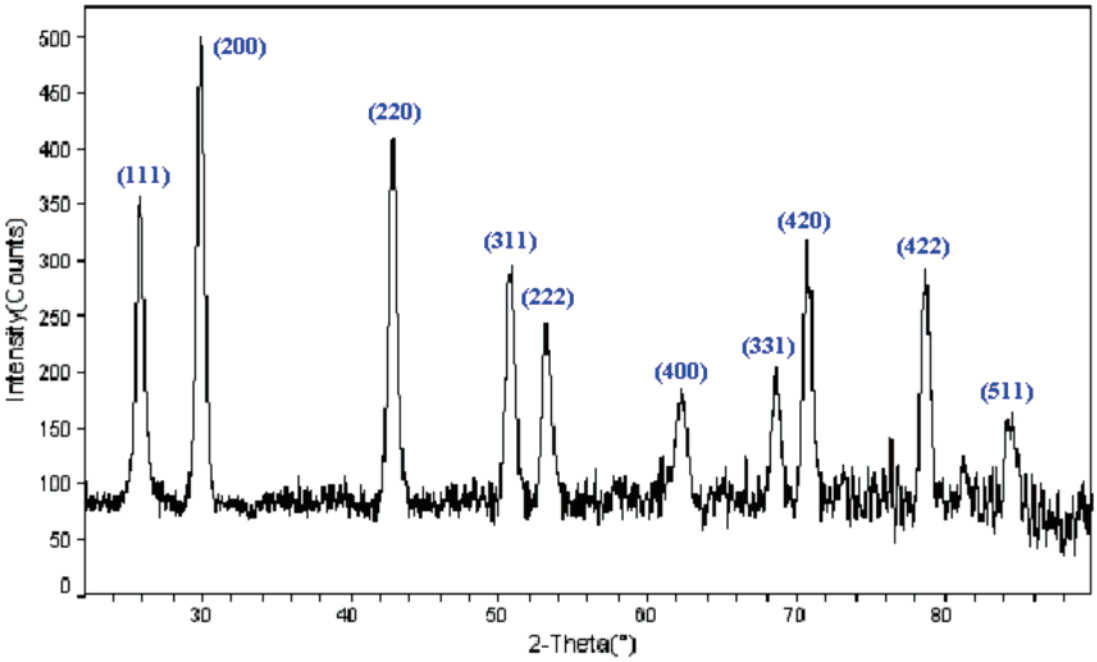

Figure 1. X-ray powder diffraction pattern of ~20 nm EuS nanoparticles.

influence the luminescence and magneto-optical properties of the europium chalcogenides which limits the extent to which these examples may be compared.[37] Important sample characteristics include capping ligand coverage, nanoparticle size, and dispersity. The nanoparticles used for the magnetic studies reported here were prepared with particular attention to optimizing these characteristics, although more work remains toward these goals. The elemental analysis is consistent with a monolayer of TOP for 18 nm nanoparticles.[38] Although the nitrogen elemental analysis was <0.5%, the UV−visible spectroscopy suggests that some phenanthroline is still present on the surface (as evidenced by a peak at ~284 nm). The FTIR of the nanoparticles indicate the presence of some oxidized trioctylphosphine (TOPO), with a small P−O stretching peak at 1466 cm^{-1}.

We have explored the effect of temperature and synthetic time on the size of the nanoparticle and found that shorter times have resulted in distinguishably smaller average particle sizes (based on X-ray diffraction 14.6 ± 0.1 nm compared with 19.1 ± 0.2), but compared with the greater size control now possible in other semiconducting systems (e.g., 1−15 nm with 1 nm increments in size developed for CdSe),[39] these have relatively broad distributions. Unlike the CdSe system where temperature appears to have a clear effect on particle size, we find that as we lower the temperature the crystallinity is so reduced that it is difficult to determine the effect of this variable on nanoparticle size. By contrast, we believe that the nature of the capping ligand is important to controlling particle size, and we are currently investigating whether the amine/phosphine ratio may play a role in determining the particle size. Amines have previously been found to mediate nanoparticle growth; for example, in the synthesis of Ag_2Se nanoparticles the ratio of [HDA]/[Precursor] was important for size control.[40]

Structure and Particle Size. Based on the X-ray powder diffraction pattern of the prepared nanoparticles, EuS was the only crystalline phase present (see Figure 1) and was indexed to the known cubic material.[41] Using the (111), (200), and (220) peaks, the fwhm was used to calculate the particle size using the Scherrer equation.[42] Based on this, the average particle was found to be 19.1 (±0.2) nm. A representative TEM image is shown in Figure 2 (with histogram inset), which was found to have an average particle size of 15 (±3) nm for measurements of ~130 individual crystallites. Although the nanoparticles exhibit solubility properties associated with capped nanoparticles, there appears to be some association of particles in the TEM images, leading to error in the size determination.

Magnetic Properties. The magnetic properties of EuS have been studied as a function of temperature (50−5 K) and field (5000−500 Oe). The magnetization as a function of temperature shows a sharp increase at low temperatures, near the T_C, similar to that observed in bulk EuS as shown in Figure 3.[43] As the field is reduced, the magnetization begins to show some evidence for peak formation (indications of a blocking temperature forming) as has been seen in other ferromagnetic nanoparticles[44] and well studied in systems such as iron.[45] This suggests that the particle size is approaching the critical

(37) Hasegawa, Y.; Thongchant, S.; Wada, Y.; Tanaka, H.; Kawai, T.; Sakata, T.; Mori, H.; Yanagida, S. *Angew. Chem., Int. Ed.* **2002**, *41* (12), 2073.
(38) The percent mass due to TOP was estimated by using the radius of the inorganic core of the nanoparticle and the density of bulk EuS (5.75 g/mL) and a shell volume estimated for a molecule layer thickness of ~10 Å and using the density of TOP (0.831 g/mL). This gave ~6% by mass of TOP compared with ~10% observed. Smaller nanoparticles have been found to have a higher ligand coverage (see: Bowen Katari, J. E.; Colvin, V. L.; Alivisatos, A. P. *J. Phys. Chem.* **1994**, *98*, 4109). Given the range of particle sizes based on TEM, this difference is not great.
(39) Murray, C. B.; Norris, D. J.; Bawendi, M. G. *J. Am. Chem. Soc.* **1993**, *115*, 8706.
(40) Ng, M. T.; Boothroyd, C.; Vittal, J. *Chem. Commun.* **2005**, *30*, 3820−3822.
(41) Nowacki, W. *Z. Kristallogr.* **1938**, *99*, 339.
(42) Bawendi, M. G.; Kortan, A. R.; Steigerwald, M. L.; Brus, L. W. *J. Chem. Phys.* **1989**, *91* (11), 7282.
(43) McGuire, T. R.; Argyle, B. E.; Shafer, M. W.; Smart, J. S. *Appl. Phys. Lett.* **1962**, *1* (1), 17.
(44) Leslie-Pelecky, D. L.; Rieke, R. D. *Chem. Mater.* **1996**, *8*, 1770.
(45) Farrell, D.; Cheng, Y.; McCallum, W. R.; Sachan, M.; Majeich, S. A. *J. Phys. Chem. B* **2005**, *109*, 13409.

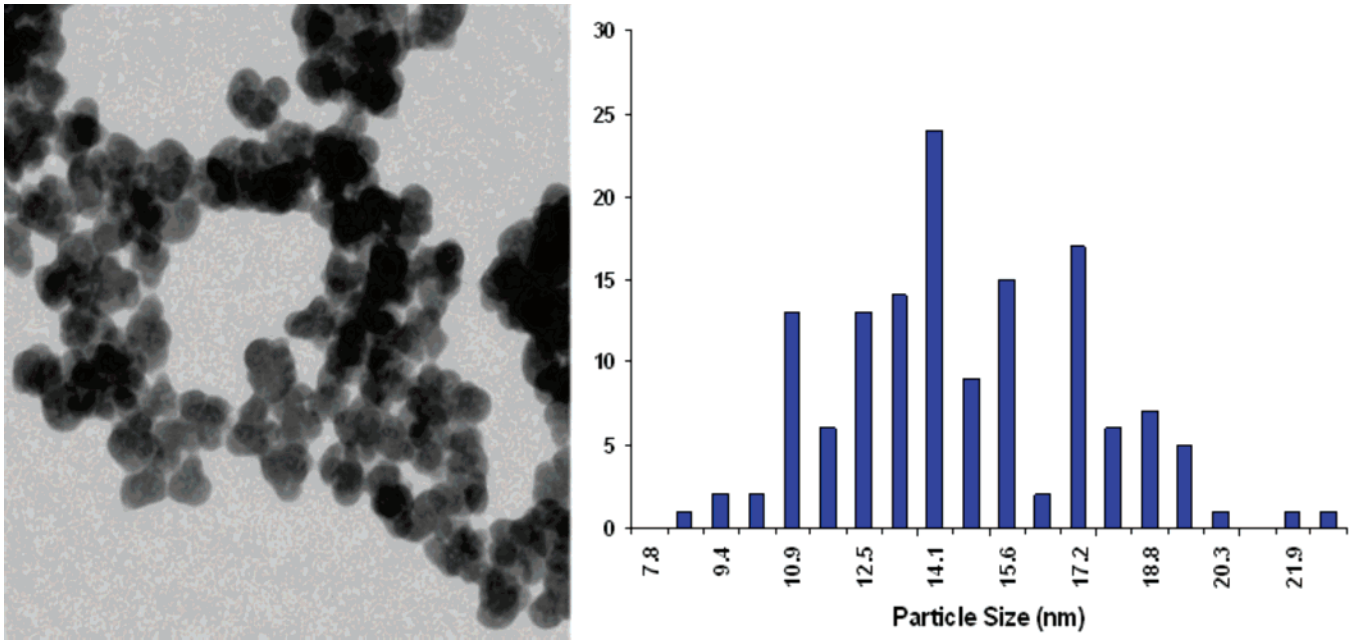

Figure 2. TEM image of EuS nanoparticles.

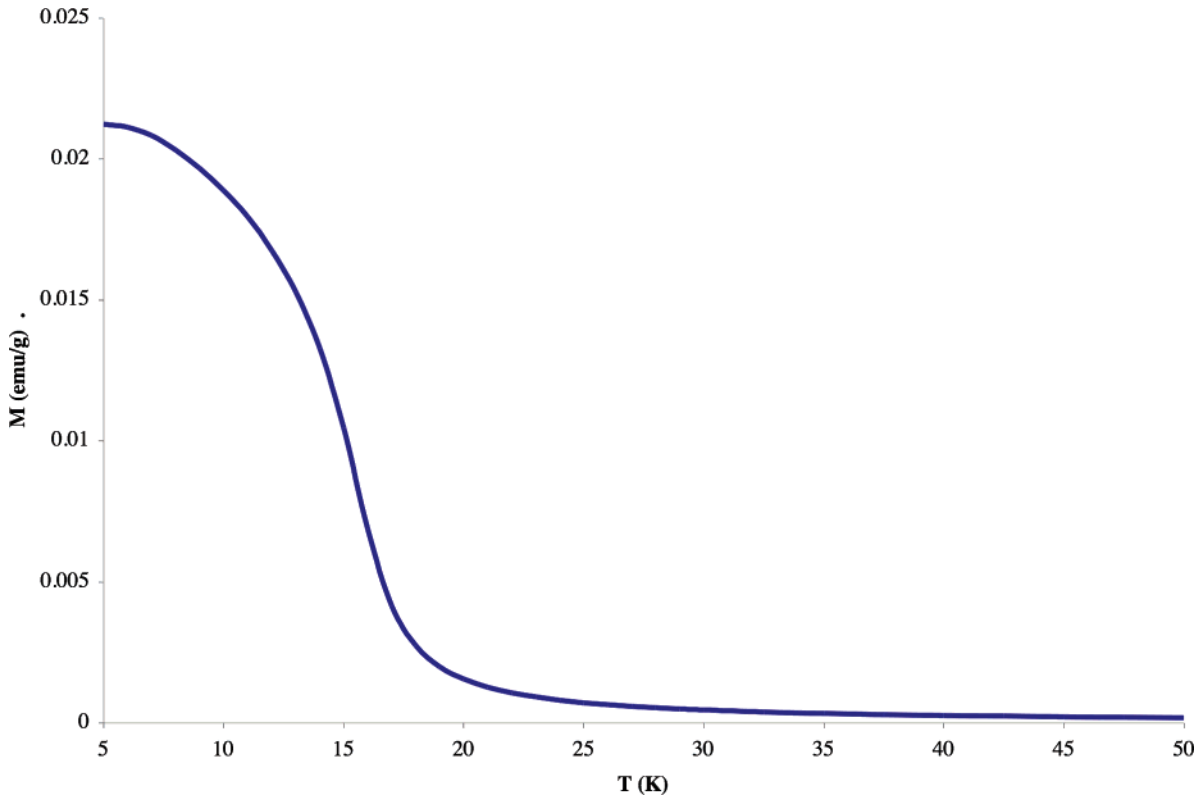

Figure 3. Magnetization as a function of temperature for 20 nm EuS nanoparticles.

dimension (D_c). At this point single domain particles are formed, where the coercive field drops to zero and the anisotropy energy is close to k_BT (i.e., superparamagnetism).[46] However, our EuS nanoparticles do not meet the two criteria for superparamagnetism, which are as follows: (1) Magnetization curves at different temperatures superimpose when M is plotted as a function of H/T and (2) Absence of hysteresis.[47] For example, in Figure 4, a small hysteresis in the magnetization as a function of field can be observed. Superparamagnetism occurs when the formation of domain walls becomes energetically unfavorable and can be estimated for materials where the crystal anisotropy is large (thus the wall energy γ is large, and the wall thickness δ is small). With moderate anisotropy such estimates become inaccurate, but the minimum D_c should be greater than δ, the domain wall thickness, which we estimated to be ~0.8 nm.[48]

(46) Spaldin, N. *Magnetic Materials: Fundamentals and Device Applications*; Cambridge University Press: 2003; p 141.
(47) Cullity, B. C. *Introduction to Magnetic Materials*; Addison-Wesley Publishing Co.: Philippines, 1972; p 410.

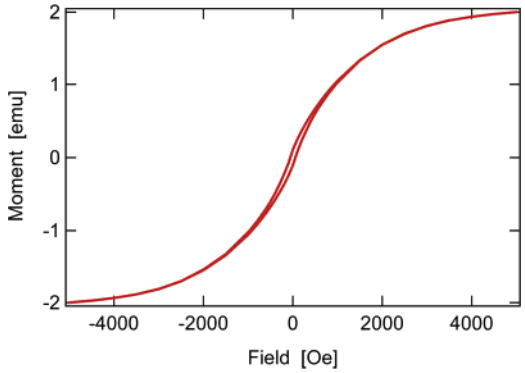

Figure 4. Magnetization as a function of field for 20 nm EuS nanoparticles.

Ferromagnetic materials exhibit spontaneous magnetization and are described by the temperature below which long range ordering occurs, the Curie temperature T_C. This transition from the magnetized to unmagnetized state is a second-order phase transition accompanied by a peak in the specific heat[49] and a sharp rise in the magnetization as the temperature is cooled below T_C.[50] Estimating the Curie temperature by extrapolating from the magnetization vs temperature curves does not provide an unambiguous determination. This type of data could be used to compare a series of samples to estimate *relative* changes in T_C; however at this time we have yet to characterize a full series of samples with appropriate steps in size. Therefore, we have used magnetic isotherms, or Arrott Plots, to provide a more sensitive and accurate measure of the Curie temperature.[51] This interpolation technique can be derived from either a Landau description of the magnetization[52] or a power series expansion of the Brillouin function[53] and is valid only in the vicinity of the Curie temperature (the "critical region"). The spontaneous magnetization (M_s) can be described by a linear equation,[54] one form[55] of which is $(H/M) = a(T - T_C) + bTM^2$, which is typically plotted as M^2 as a function of H/M at constant temperature (as we have done in Figure 5). Often isotherms will bend at higher and lower temperatures (if the field is low enough) due to magnetic anisotropy.[56] Because spontaneous magnetization is a slowly varying function except within the limits $H \rightarrow 0$ and $T - T_C \rightarrow 0$,[57] the bending is most pronounced at low fields and low temperatures. Thus, typically the high field data are extrapolated for temperatures below T_C.[58] The intercept of these isotherms with the *y*-axis (i.e., where $M_s^2 = 0$) should be positive if $T > T_C$ and negative if $T < T_C$. This can be seen qualitatively in Figure 5, where clearly the high field data for $T = 14$ and 15 K have a negative intercept and those for $T = 16$ K have a positive intercept placing T_C between 15 and 16 K. The Curie point is determined by first finding the zero field limit as the intercept on the M^2 axis when extrapolated to $H/M = 0$. This value of M_s^2 for each temperature is plotted in Figure 6. The Curie temperature is defined as the temperature where M_s^2 is zero (crosses the *x*-axis). For 19.1 nm particles, we determine a $T_C = 15.2$ K, which is depressed from that of bulk EuS (16.6 K), as shown in Figure 6.

In our initial studies of the size dependence of EuS nanoparticles, we have found for a second sample, with a smaller average particle size of 14.6 (±0.1) nm based on X-ray powder diffraction, an enhanced decrease in the Curie temperature. Using a similar Arrott analysis we determined a T_C of 14.6 K (shown in Figure 6). Our first observation is that TEM measurements suggest a relatively broad particle size range (10 ± 2 nm), and based on these data the two samples would appear to be indistinguishable. However, the X-ray powder diffraction is consistent with the more sensitive magnetic measurements that suggest that these are statistically different in their average size. Second, these data support the hypothesis that the Curie temperature decreases as the particle size decreases.

There are three mechanisms we have considered to explain the decrease in ordering temperature for a decrease in nanoparticle size: strain, surface effects, and band gap changes. Recent work on EuS thin films and multilayers have shown that, depending on the substrate, the T_C can vary between +1 and −3 K as a result of substrate induced lattice strain.[59] This is likely reflected in changes to the orbital overlap term *b*, in eq 2, due to expansion or compression of atomic distances. Although this is well within the range of T_C changes we have observed, the question is whether the surface strain in nanoparticles is comparable. Studies of CdSe and CdS using EXAFs suggest there is only very weak static strain in semiconductor nanoparticles, with atomic distances (mean-square relative displacements) close to that of the bulk.[60] We do not see shifts in the diffraction peaks, which would suggest uniform strain, and it is difficult to separate line broadening due to nonuniform strain and that due to particle size. Characterization of microstructure from line-broadening analysis can be carried out using Rietveld analysis, Williamson−Hall plots, or Fourier methods such as that of Warren−Averbach.[61] We are currently investigating which method is most appropriate for nanoparticles. We also anticipate that the capping ligand should prevent surface reconstruction, although this is by analogy to thin films and we have no formal evidence for this.

A second mechanism can be derived based on the fact that nanoparticles have increased numbers of surface atoms. Studies of ferromagnetic thin films have found competing forces due to reduced coordination of atoms at the surface. The reduced coordination at the surface can result in the loss of near-neighbor coupling (which can lower T_C) and enhanced the surface magnetic moment (which can increase T_C).[62] However, studies of the critical behavior of EuS thin films using spin-polarized low-energy electron diffraction found no change in T_C of the

(48) Domain wall thickness can be estimated as $\pi = (0.3k_BT_C\pi^2/3Ka)^{1/2}$ where T_C is the Curie temperature, k_B is Boltzman's constant, K is the anisotropy constant, and a is the lattice constant (from Cullity, B. ibid, p 291).
(49) Kraftmakher, Y. *Eur. J. Phys.* **1997**, *18*, 448.
(50) West, A. *Solid State Chemistry and Its Applications*; Wiley and Sons: New York, 1984; p 553.
(51) Arrott, A. *Phys. Rev.* **1957**, *108* (6), 1394.
(52) Neumann, K. U.; Ziebeck, K. R. A. *J. Magn. Magn. Mater.* **1995**, *140*−*144*, 967.
(53) Aharoni, A. *Introduction to the Theory of Ferromagnetism*; Oxford Science Publications: 2000, U.K.; p 80.
(54) Chikazumi, *S. Physics of Ferromagnetism*; Oxford Science: Oxford, 2000; p 118.
(55) Aharoni, A. *Introduction to the Theory of Ferromagnetism*; Oxford Science Publications: 2000, U.K.; p 80.
(56) Noakes, J. E.; Arrott, A. *J. Appl. Phys.* **1967**, *38*, 973.
(57) Arrott, A.; Noakes, J. E. *Phys. Rev. Lett.* **1967**, *19* (14), 786.
(58) Saito, H.; Zayets, V.; Yamagata, S.; Ando, K. *Phys. Rev. Lett.* **2003**, *90* (20), 207202-1.
(59) (a) Swikowicz, R.; Story, T. *J. Phys.: Condens. Matter* **2000**, *12*, 8511. (b) Stachow-Wojcik, A.; Story, T.; Dobrowolski, W.; Arciszewska, M.; Galazka, R. R.; Kreijveld, M. W.; Swuste, C. H. W.; Swagten, H. J. M.; de Jong, W. J. M.; Twardowski, A.; Sipatov, A. Y. *Phys. Rev. B* **1999**, *60* (22), 15220.
(60) Marcus, M.; Flood, W.; Stiegerwald, M.; Brus, L.; Bawendi, M. *J. Phys. Chem.* **1991**, *95*, 1572.
(61) (a) Warren, B. E. *X-ray Diffraction*; Addison-Wesley: Reading, MA 1969. (b) Langford, J. I.; Louer, D. *Rep. Prog. Phys.* **1996**, *59*, 131.
(62) Jensen, P. J.; Bennemann, K. H. *Langmuir*, **1996**, *12*, 45.

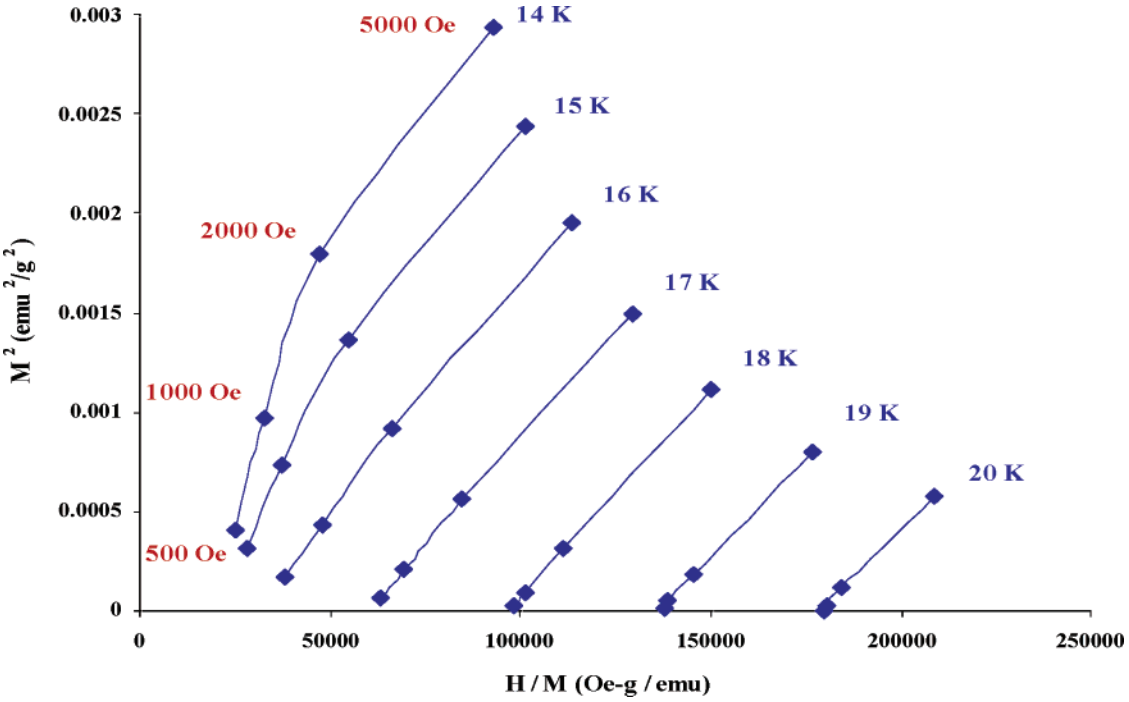

Figure 5. Arrott plot of 20 nm EuS nanoparticles (M^2 vs (H/M) isotherms).

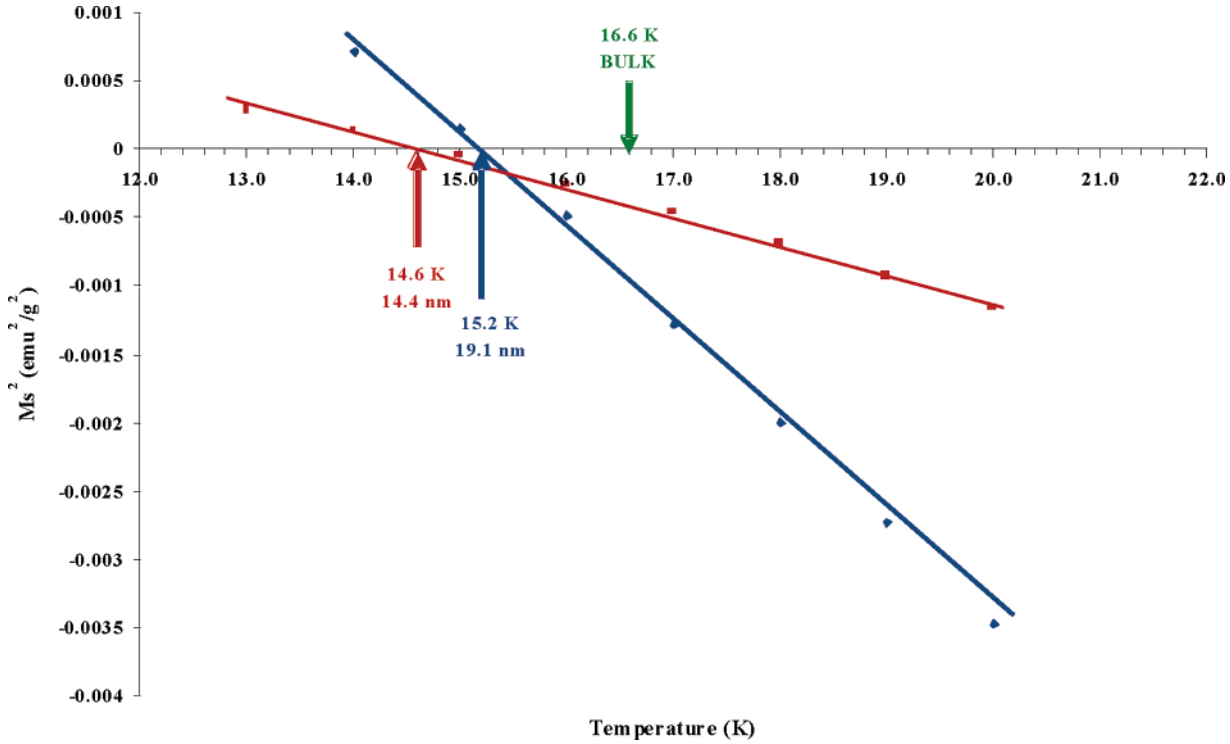

Figure 6. Comparison of T_C obtained for 14.4 nm EuS nanoparticles (red), 19.1 nm EuS nanoparticles (blue), and bulk EuS (green).

surface compared with the bulk.[63] Nonetheless, a second explanation for the reduced T_C is the loss of near neighbors, lowering the average $\bar{Z}_1$ and $\bar{Z}_2$. For a 20 nm spherical particle, approximately 10% of the atoms are at the surface. Assuming the coordination number of surface atoms is half that of the bulk, one can estimate an average of neighbors for surface and bulk atoms as $\bar{Z}_1 \approx 11.4$, and $\bar{Z}_2 \approx 5.7$. Using a modification[64] of eq 1:

$$T_C = T_C^{\text{bulk}} \left| \frac{\bar{z}_1 J_1 + \bar{z}_2 J_2}{12 J_1 + 6 J_2} \right|$$

we calculate a $T_C \approx 15.8$ K, which is close to that observed.

Finally, the third model (and our initial hypothesis) is that J_1 is altered by changes in the band gap. Knowing the band gap and using eq 2, one can estimate changes in J_1 assuming that

(63) Dauth, B. H.; Alvarado, S. F.; Campagna, M. *Phys. Rev. Lett.* **1987**, *58* (20), 2118.

the terms A (4f valence to 5d conduction band exchange) and b (orbital overlap) are unaltered by size. Generally, increasing the E_g will reduce J_1 and lower the ordering temperature, which is consistent with the observed trend that T_C decreases as particle size decreases. The primary weakness in this analysis is determining an accurate measure of the E_g. In addition to the similar ambiguities of determining an absorption edge, there is some question of assigning the transitions in these materials. The optical properties of bulk EuS are complicated by changes that occur with temperature and magnetic field.[65] The absorption spectra have historically been interpreted as having a small absorption centered around the $4f-5dt_{2g}$ transition with a more intense broad absorption due to the transition from the 4*f* to 6*s* band. There are inconsistencies over peak assignments in both thin films and nanoparticles,[66] which may be related to purity or surface defects. These nanoparticles show an absorption at 520 nm, which if we assign this to the $4f-5dt_{2g}$ transition, gives a band gap of 2.39 eV. This value is surprisingly large, given our estimate of the exciton Bohr radius of approximately 5.8 nm, smaller than the nanoparticles reported here.[67] Using this value, nonetheless, to estimate J_1, we obtain 0.109, which would give a calculated approximation of $T_C \approx 7$ K (using eq 1), which is far lower than what we observe.

Several questions remain from this work. The most critical question, which may help distinguish between the possibilities outlined above, is what is the functional relationship between the decrease in T_C and particle size? If it depends on the number of surface atoms, it should vary as $1/R$ (R being the radius of the particle), whereas if the E_g has an important role, the T_c should vary as a function of $1/E_g^2$. Also important is the question of assigning the electronic transitions in these nanoparticles. If the peak at 520 nm is the optical band gap, it ought to vary with nanoparticle radius, according to the Brus equation. We have observed changes in intensity of this peak but not position for different synthetic conditions. This would be the case if we are not yet close to the Bohr radius or if this is not due to the band gap. If it is a result of surface defects, or oxidation at the surface, it should be possible to determine this by varying the capping ligand or by forming core/shell type nanoparticles. For example, a shell layer of PbS, which has a close lattice match for EuS (PbS $a \approx 5.94$ Å and EuS $a \approx 5.97$ Å),[68] should identify whether surface states are responsible for this absorption.[69] We are currently using room-temperature europium Mossbauer spectroscopy to determine the coordination environment of the europium in these nanoparticles.

Conclusions

In this work we have studied the effect of particle size on the magnetic ordering temperature in lanthanide magnetic semiconductors. Our evidence suggests there is a lowering in the ferromagnetic Curie temperature with decreasing particle size. Further experiments with a series of controlled particle sizes (with a more narrow size distribution within a sample) should distinguish whether strain, surface effects, or band gap changes are responsible for the changes in strength of the magnetic coupling.

Acknowledgment. We thank the National Science Foundation for funding this work (NER: 0304273, CAREER: 0449829), and Brad Lewis would like to thank Tom Mallouk for support.

Supporting Information Available: The optical spectroscopy of the nanoparticles, bulk materials, and theoretical assignment of transitions are compared in S1−S3. This material is available free of charge via the Internet at http://pubs.acs.org.

JA0620080

(64) Stachow-Wojcik, A.; Story, T.; Dobrowolski, W.; Arciszewska, M.; Galazka, R. R.; Kreijveld, M. W.; Swuste, C. H. W.; Swagten, H. J. M.; de Jong, W. J. M.; Twardowski, A.; Sipatov, A. Y. *Phys. Rev. B* **1999**, *60* (22), 15220.
(65) Busch, G.; Wachter, P. *Phys. Kondens. Mater.* **1966**, *5*, 232.
(66) Thongchant, S.; Hasegawa, Y.; Wada, Y.; Yanagida, S. *J. Phys. Chem. B* **2003**, *107*, 2193−2196.
(67) Using the approach of L. E. Brus (*J. Chem. Phys.* **1984**, *80* (9), 4403), where the m_h^* is neglected (assuming is it much larger than m_e^*), m_e^* is 0.456, and the dielectric constant ϵ_0 is 10 (from Umehara, M. *Phys. Rev. B* **2002**, *65*, 205208).
(68) Stachow-Wojcik, A.; Story, T.; Dobrowolski, W.; Arciszewska, M.; Galazka, R. R.; Kreijveld, M. W.; Swuste, C. H. W.; Swagten, H. J. M.; de Jong, W. J. M.; Twardowski, A.; Sipatov, A. Y. *Phys. Rev. B* **1999**, *60* (22), 15220.
(69) Kuno, M.; Lee, J. K.; Dabbousi, B. O.; Mikulec, F. V.; Bawendi, M. G. *J. Chem. Phys.* **1997**, *106* (23), 9869.